

UNIVERSIDAD DE CONCEPCIÓN



CENTRO DE INVESTIGACIÓN EN
INGENIERÍA MATEMÁTICA (CI²MA)



A model of clarifier-thickener control with time-dependent feed
properties

FERNANDO BETANCOURT, RAIMUND BÜRGER,
STEFAN DIEHL, SEBASTIAN FARÅS

PREPRINT 2013-18

SERIE DE PRE-PUBLICACIONES

A MODEL OF CLARIFIER-THICKENER CONTROL WITH TIME-DEPENDENT FEED PROPERTIES[†]

FERNANDO BETANCOURT^{A,*}, RAIMUND BÜRGER^B, STEFAN DIEHL^C,
AND SEBASTIAN FARÁS^C

ABSTRACT. A one-dimensional model of the process of continuous sedimentation in a clarifier-thickener unit is presented. The model is expressed as a system of two nonlinear partial differential equations describing the solids volume fraction and the varying settling velocity of the solids as functions of depth and time. The governing model extends the well-known model for the dynamics of a flocculated suspension in a clarifier-thickener advanced by Bürger, Karlsen and Towers [SIAM J. Appl. Math. 65 (2005) 882–940]. Operating charts are calculated to be used for the control of steady states, in particular, to keep the sediment level and the underflow volume fraction at desired values. A numerical scheme and a simple regulator are proposed and numerical simulations are performed.

1. INTRODUCTION

1.1. **Scope.** Water consumption has become an important problem in the mineral processing industry, especially for countries where most plants are located in desert areas. The necessity to increase the capacity of many metals concentrators, led by higher metal prices, calls for additional efforts in recovering the maximum possible amount of water in solid-liquid separation of the suspensions arising as tailings from the stage of froth filtration. Thickeners are widely used as a first stage in this process. They operate continuously, producing a concentrated underflow while particle-free supernatant water overflows. This principle is well explained in handbook entries (Osborne, 1981; Fitch, 1993; Chapter 18 of Perry et al., 1998; Chapter 15 of Wills and Napier-Munn, 2006). Thickeners are equipped with a rake mechanism that helps moving the sediment to the underflow outlet. The rake drive provides torque to move the rake arms against the resistance exerted by the thickened material. Due to limitations of the available torque and to protect the rake, one wishes to control the operation of a thickener in such a way that the sediment level is kept at a relatively small fraction, say 30%, of the thickener height. In fact, a failure in the drive equipment generally means that the thickener has to be dug out (Schoenbrunn and Laros, 2002).

Date: August 1, 2013.

[†]Presented at *Physical Separation '13*, Falmouth, UK, June 20 and 21, 2013.

*Corresponding author.

^ADepartamento de Ingeniería Metalúrgica, Facultad de Ingeniería, Universidad de Concepción, Casilla 160-C, Concepción, Chile. E-Mail: fbetancourt@udec.cl.

^BCI²MA and Departamento de Ingeniería Matemática, Facultad de Ciencias Físicas y Matemáticas, Universidad de Concepción, Casilla 160-C, Concepción, Chile. E-Mail: rburger@ing-mat.udec.cl.

^CCentre for Mathematical Sciences, Lund University, P.O. Box 118, S-221 00 Lund, Sweden. E-Mail: diehl@maths.lth.se, faras@maths.lth.se.

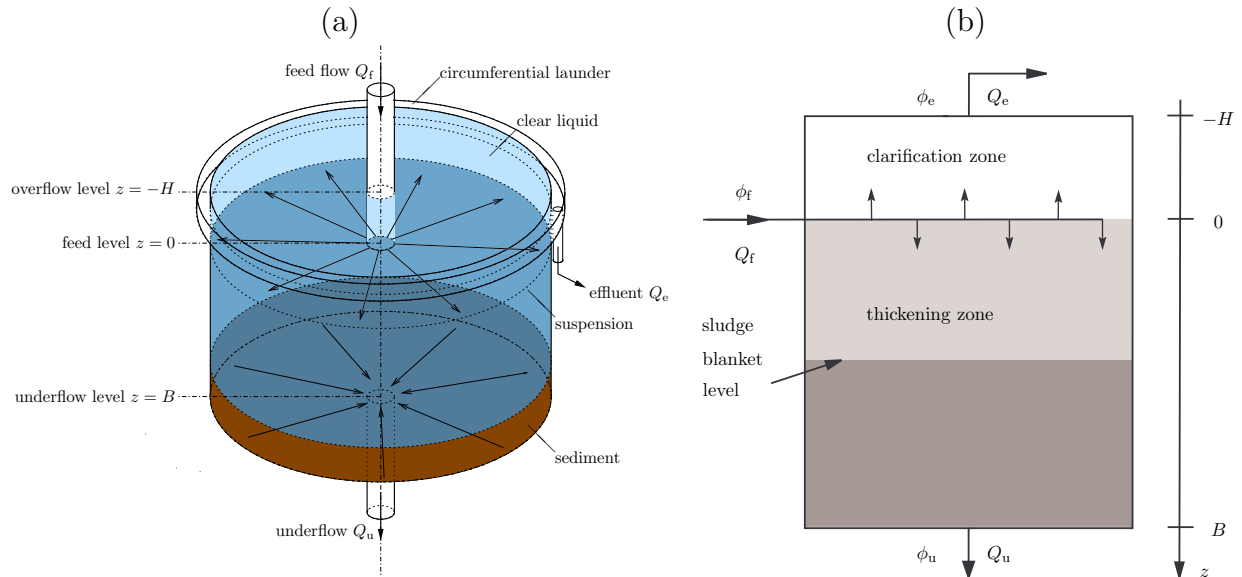


FIGURE 1. Schematic illustrations of the clarifier-thickener (CT): (a) principle of operation, (b) idealized one-dimensional model. The height of the clarification zone is denoted by H and the depth of the thickening zone by B . The indices of the volume fractions (ϕ) and volumetric flows (Q) stand for $f =$ feed, $e =$ effluent and $u =$ underflow.

Furthermore, the performance of a thickener depends on the settling velocity of solid particles. This velocity depends on the size of the particles and in the density difference between solids and liquid. For mono-sized spherical particles of diameter \mathcal{D} and density ρ_s settling in an unbounded fluid of density ρ_f and viscosity μ_f , the settling velocity is given by the Stokes velocity

$$v_{St} = \frac{\mathcal{D}^2(\rho_s - \rho_f)g}{18\mu_f}, \quad (1)$$

where g is the acceleration of gravity. In fact, to maximize the recovery in the flotation process, mineral particles are reduced in size in crushers and mills before entering flotation to sizes of 50–200 μm . The small particle sizes constitute a challenge for the dewatering stages since particles settle very slowly. Usually the effective particle sizes, thereby the settling velocities, are increased by flocculation. This is achieved by addition of a flocculant, which causes small particles to aggregate into large units, called flocs. Since the flocculation process is fairly rapid, the dosage of the flocculant added to the feed suspension can be regarded as an independent variable that can be adjusted for purposes of thickener control, for example with the aim to maintain the sediment level at constant height, in response to variations of the solid feed flux and concentration which cannot be controlled. It is the purpose of this paper to introduce a new model for thickener simulation and control that explicitly includes variations in the state of flocculation as an additional control variable.

A seminal work in thickener modelling is the kinematic theory by Kynch (1952), which describes the batch settling of an ideal suspension of small, equal-sized rigid spheres in a viscous fluid. Numerous studies (see Concha and Bürger, 2002, 2003 for historical overviews) and extensive use in industry made this theory a powerful tool to model and design settling equipments (Concha and Barrientos, 1993). Bürger et al. (2005) extended the Kynch theory to a complete model of a continuous thickener by including sediment compressibility and modeling the feed, overflow and discharge mechanisms by discontinuous spatial variations in the bulk flows and a singular source term. This model corresponds to a simplified, spatially one-dimensional setup (see Figure 1). The model is described by the following nonlinear partial differential equation (PDE) for the volume fraction of solids ϕ as a function of depth z and time t (Bürger et al. 2005, 2011, 2012):

$$\frac{\partial \phi}{\partial t} + \frac{\partial}{\partial z} F(\phi, z, t) = \frac{\partial}{\partial z} \left(\gamma(z) d(\phi) \frac{\partial \phi}{\partial z} \right) + \frac{Q_f(t) \phi_f(t)}{A} \delta(z). \quad (2)$$

The convective flux function F incorporates the in- and outgoing bulk flows of the vessel and a constitutive assumption on the hindered settling flux. The compression of solids at high concentrations is modelled by the term containing the function d which includes a constitutive assumption on the effective solid stress function. The source term models the feed inlet located at $z = 0$. In contrast to previous models that include the thickening zone only and describe the feed, discharge and overflow mechanisms by boundary conditions (Shannon and Tory, 1966; Petty, 1975; Bustos et al., 1990a, 1990b, 1999; Concha and Bustos, 1992), the model based on (2) includes a clarification zone, located above the thickening zone (see Figure 1), which may handle situations of thickener overload and permits to describe the high-rate mode of operation (i.e., when the sediment level is located above the feed source). To be consistent with previous treatments, we refer to a thickener described by Figure 1 and modeled by (2) as a clarifier-thickener (CT).

In this work, we present an extension of the CT model developed by Bürger et al. (2005) taking into account changes in the physical properties of the solid particles that are fed to the CT. The extension can be posed as an additional partial differential equation that describes a scalar quantity which corresponds to the free settling velocity determined by the state of flocculation of the solids particles. Roughly speaking, this quantity may be interpreted as the flocculant concentration, and it passively travels with the solids particles. Moreover, a simple regulator, a numerical scheme and simulation examples are shown.

1.2. Related work. To put this paper further in the proper perspective, we recall that the flocculation process consists of 3 steps (Hogg, 2000), namely (i) destabilization of suspended particles, (ii) floc formation and growth and (iii) floc degradation. Step (i) is usually controlled by pH modifications. In mineral processing, step (ii) consists of the adsorption of fine particles in high molecular weight polymer, also called bridging flocculation (Hogg, 2013). The adsorption rate is determined by particle-polymer collisions. The most important way in which particles are brought into contact with the polymer is due to the fluid motion (orthokinetic flocculation) (Gregory, 2005; McFarlane et al., 2005). It is well known that the number of collisions is proportional to the shear rate of the suspension, the concentration of solid particles and flocculant concentration. However, floc degradation is also related to

shear and then there is a trade-off between floc formation and floc degradation in agitated suspensions. To avoid this problem, normally, the used shear rate in flocculation steps is less than 100 s^{-1} .

The authors are well aware that flocculation is a complex operation, which is however not part of the model. Rather, we assume that the settling velocity of a single particle (floc) that enters the CT, v_{St} , is an explicit known function of the (properly normalized) flocculant concentration c , i.e. $v_{\text{St}} = v_{\text{St}}(c)$. Experimental information that helps to provide this relationship includes the papers by Ye et al. (1998), Aziz et al. (2000), Besra et al. (1996), Glover et al. (2000, 2004), Balastre et al. (2002), Jin et al. (2003), Zhao (2004), Chen et al. (2007), McGuire et al. (2008), Chakrabarthy et al. (2008), Kourki and Famili (2012) and Eswaraiyah et al. (2012).

The available model by Bürger et al. (2005), which gives rise to the governing equation (2), combines several non-standard mathematical properties, including the appearance of discontinuous solutions, discontinuities in the definition of the flux F with respect to z , and the fact that the sediment compressibility function $d = d(\phi)$ becomes zero whenever the volume fraction ϕ is smaller than a critical concentration (or gel point) ϕ_c . The latter properties means that the second-order PDE (2) degenerates into a first-order PDE wherever $\phi \leq \phi_c$, where the location of the type-change interface $\phi = \phi_c$, that is, the sediment level, is unknown beforehand. While Bürger et al. (2005) provide the full mathematical detail including a numerical scheme and the corresponding convergence analysis, particularly accessible introductions to the model formulation and mathematical treatment are provided by Bürger et al. (2011) and Diehl (2012). A hands-on description of a numerical scheme for the approximate solution of (2), and therefore for the simulation of the dynamics of a clarifier-thickener, is given by Bürger et al. (2013).

As for the control of CTs modelled by PDEs, we refer to Barton et al. (1992), Chancelier et al. (1994), Diehl (2006, 2008), Bürger and Narváez (2007), Betancourt et al. (2013) and Diehl and Farås (2013).

The basic novelty in terms of the governing equations is an additional PDE that describes the transport of a scalar quantity that reflects a variable property by which the solid particles entering the CT are “marked”, and which in general influences the rheology of the suspension. A similar concept, though in a more involved model, was advanced by Lester et al. (2010). Their so-called microstructural parameter χ is an abstract quantity that represents the thixotropic state of the suspension, and which is advocated with the solids phase velocity.

1.3. Outline of the paper. This paper is organized as follows: Section 2 describes the phenomenological model and its relation with flocculation. Section 3.1 describes the steady-state solution of the model and some operating charts for control of steady-state solutions. The proposed numerical scheme is given in the Appendix. Section 4 is devoted to numerical simulations. Finally, in Section 5, conclusions are given and future research is outlined.

2. MATHEMATICAL MODEL

We consider an idealized CT shown in Figure 1 with the volumetric overflow or effluent rate $Q_e \geq 0$, the volumetric discharge or underflow rate $Q_u \geq 0$, the volume feed rate

$Q_f = Q_u + Q_e$, and the feed, underflow and effluent solids volume fractions ϕ_f , ϕ_u and ϕ_e . The downward-pointing z -axis can be divided into the effluent zone ($z < -H$), the clarification zone ($-H < z < 0$), the thickening zone ($0 < z < B$), and the underflow zone ($z > B$). We assume that the cross-sectional area is constant (denoted by A) and that the solids volume fraction ϕ only depends on depth z and time t .

2.1. Model for non-varying feed properties (Bürger et al., 2005). The conservation of mass yields the PDE (2), where the convective flux function is

$$F(\phi, z, t) := \begin{cases} -Q_e(t)\phi/A & \text{for } z < -H, \\ -Q_e(t)\phi/A + v_{hs}(\phi)\phi & \text{for } -H \leq z < 0, \\ Q_u(t)\phi/A + v_{hs}(\phi)\phi & \text{for } 0 < z \leq B, \\ Q_u(t)\phi/A & \text{for } z > B, \end{cases} \quad (3)$$

which involves the hindered settling velocity function

$$v_{hs}(\phi) := v_{St}V(\phi), \quad (4)$$

where V is a dimensionless constitutive function modelling the hindered effect satisfying $V(0) = 1$. In mineral processing, the expression by Richardson and Zaki (1954)

$$V(\phi) = (1 - \phi)^{n_{RZ}}$$

with $n_{RZ} > 1$ is often used. The function $d = d(\phi)$ describing sediment compressibility is given by Bürger et al. (2005):

$$d(\phi) := \frac{v_{hs}(\phi)\sigma'_e(\phi)}{(\rho_s - \rho_f)g}, \quad (5)$$

where σ_e is the effective solid stress function, whose derivative satisfies

$$\sigma'_e(\phi) \begin{cases} = 0 & \text{for } 0 \leq \phi < \phi_c, \\ > 0 & \text{for } \phi > \phi_c, \end{cases}$$

where ϕ_c is the material-dependent critical concentration. A typical effective solid stress function is given by

$$\sigma_e(\phi) = \begin{cases} 0 & \text{for } \phi < \phi_c, \\ \alpha \exp(\beta\phi) & \text{for } \phi \geq \phi_c, \end{cases}$$

where α [Pa] and β are parameters that can be determined through experiments (Garrido et al., 2000). The function $\gamma = \gamma(z)$ appearing in the right-hand side of (2) indicates whether z is inside or outside of the CT, i.e.,

$$\gamma(z) := \begin{cases} 1 & \text{for } -H \leq z \leq B, \\ 0 & \text{for } z < -H \text{ or } z > B. \end{cases} \quad (6)$$

The outlet concentrations at the effluent and underflow are given by the respective expressions

$$\phi_e(t) := \phi(-H^-, t), \quad \phi_u(t) = \phi(B^+, t).$$

Here the notation $\phi(-H^-, t)$ indicates that we take the limit of $\phi(z, t)$ as z approaches $-H$ from above ($z < -H$), corresponding to the exterior of the CT. Likewise, $\phi(B^+, t)$ means that we take the limit $z \rightarrow B$ from below ($z > B$). Both notations consider that the solution $\phi = \phi(z, t)$ is, in general, discontinuous at $z = -H$ and $z = B$.

The definition of the function F in (3) in combination with (6) implies that outside the CT, the solid and liquid phases move at the same velocity, i.e. the suspension is just advected away from the CT.

2.2. Model for varying feed properties. Suppose now that some property of the solids that are fed to the CT changes with time. This property may be the colour of the particles or, which we are interested in, the sedimentation velocity of each particle defined by the flocculant dosage. We let $k = k(z, t)$ denote a positive dimensionless number describing such a property at the depth z and time t within the CT. For a grey scale, k could be a number between zero and one. For a varying settling velocity, $k = 0$ means a zero particle settling velocity and $k = 1$ the maximal possible velocity, which occurs when the suspension is flocculated in the optimal way, possibly by adding an adequate dosage of flocculant. If the parameter v_0 denotes such a maximal velocity for a single particle, then the single settling velocity v_{st} should in the model be replaced by $k(z, t)v_0$. Hence, the constitutive function (4) should be replaced by

$$\overline{v}_{\text{hs}}(\phi, k) := kv_0V(\phi) = kv_{\text{hs}}(\phi). \quad (7)$$

Replacing $v_{\text{hs}}(\phi)$ in (5) by $\overline{v}_{\text{hs}}(\phi, k)$, we obtain the new diffusion coefficient

$$\overline{d}(\phi, k) := \frac{kv_{\text{hs}}(\phi)\sigma'_e(\phi)}{(\rho_s - \rho_f)g} = kd(\phi),$$

and Equation (2) becomes

$$\frac{\partial \phi}{\partial t} + \frac{\partial}{\partial z}(\overline{F}(\phi, k, z, t)) = \frac{\partial}{\partial z} \left(\gamma(z)k \frac{\partial D(\phi)}{\partial z} \right) + \frac{Q_f(t)\phi_f(t)}{A} \delta(z), \quad (8)$$

where we have redefined F as follows:

$$\overline{F}(\phi, k, z, t) := \begin{cases} -Q_e(t)\phi/A & \text{for } z < -H, \\ -Q_e(t)\phi/A + kv_{\text{hs}}(\phi)\phi & \text{for } -H \leq z < 0, \\ Q_u(t)\phi/A + kv_{\text{hs}}(\phi)\phi & \text{for } 0 < z \leq B, \\ Q_u(t)\phi/A & \text{for } z > B, \end{cases}$$

and we define

$$D(\phi) := \int_0^\phi d(s) ds.$$

In the feed inlet, the time variation of the property is described by $k_f = k_f(t) \in [0, 1]$. The feed flux of particles carrying the property $k_f(t)$ at time t is $k_f(t)\phi_f(t)Q_f(t)$. To formulate an equation for the depth and time variation of $k(z, t)$, we postulate that

$$w(z, t) := k(z, t)\phi(z, t)$$

is the density of a conserved quantity. Consider an arbitrary interval of the depth axis, (z_1, z_2) , and let $\Phi|_{z=z_1}$ denote the total flux per area unit of particles passing $z = z_1$. The flux of the property k across $z = z_1$ at time t is then $Ak\Phi|_{z=z_1}$. The Reynolds Transport Theorem then yields

$$\frac{d}{dt} \int_{z_1}^{z_2} Ak(z, t)\phi(z, t) dz = A((k\Phi)|_{z=z_1} - (k\Phi)|_{z=z_2}) + \int_{z_1}^{z_2} k_f(t)Q_f(t)\phi_f(t)\delta(z) dz,$$

where the total flux Φ is given by

$$\Phi \left(\phi, \frac{\partial \phi}{\partial z}, k, z, t \right) = \bar{F}(\phi, k, z, t) - \gamma(z)k \frac{\partial D(\phi)}{\partial z}.$$

This yields the PDE

$$\frac{\partial(k\phi)}{\partial t} + \frac{\partial}{\partial z} (k\bar{F}(\phi, k, z, t)) = \frac{\partial}{\partial z} \left(\gamma(z)k^2 \frac{\partial D(\phi)}{\partial z} \right) + \frac{Q_f(t)k_f(t)\phi_f(t)}{A} \delta(z), \quad (9)$$

which together with (8) constitutes our model. Defining $w_f := k_f\phi_f$ we arrive at the following system of conservation equations:

$$\frac{\partial \phi}{\partial t} + \frac{\partial}{\partial z} (\bar{F}(\phi, w/\phi, z, t)) = \frac{\partial}{\partial z} \left(\gamma(z) \frac{w}{\phi} \frac{\partial D(\phi)}{\partial z} \right) + \frac{Q_f(t)\phi_f(t)}{A} \delta(z), \quad (10)$$

$$\frac{\partial w}{\partial t} + \frac{\partial}{\partial z} \left(\frac{w}{\phi} \bar{F}(\phi, w/\phi, z, t) \right) = \frac{\partial}{\partial z} \left(\gamma(z) \frac{w^2}{\phi^2} \frac{\partial D(\phi)}{\partial z} \right) + \frac{Q_f(t)w_f(t)}{A} \delta(z). \quad (11)$$

The final form, which we will also refer to in the numerical discretization, is obtained by introducing the bulk velocity function:

$$q(z, t) := \begin{cases} -Q_e(t)/A & \text{for } z < 0, \\ Q_u(t)/A & \text{for } z > 0, \end{cases}$$

incorporating the source terms into the convective flux by writing $\delta(z) = H'(z)$, where H is the Heaviside step function, and noting that for $\phi > 0$ and any number p we have

$$\frac{1}{\phi^p} \frac{\partial D(\phi)}{\partial z} = \frac{\partial D_p(\phi)}{\partial z}$$

for $p = 1, 2$, where

$$D_p(\phi) := \int_0^\phi \frac{d(s)}{s^p} ds.$$

This gives

$$\frac{\partial \phi}{\partial t} + \frac{\partial}{\partial z} (q(z, t)(\phi - \phi_f) + \gamma(z)k(\phi, w)v_{\text{hs}}(\phi)\phi) = \frac{\partial}{\partial z} \left(\gamma(z)w \frac{\partial D_1(\phi)}{\partial z} \right), \quad (12)$$

$$\frac{\partial w}{\partial t} + \frac{\partial}{\partial z} (q(z, t)(w - w_f) + \gamma(z)k(\phi, w)v_{\text{hs}}(\phi)w) = \frac{\partial}{\partial z} \left(\gamma(z)w^2 \frac{\partial D_2(\phi)}{\partial z} \right), \quad (13)$$

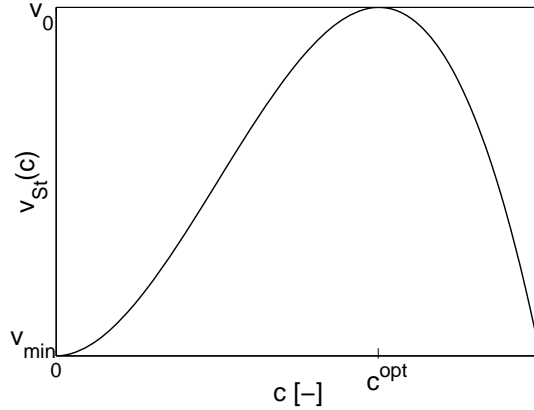


FIGURE 2. Schematic graph of the unimodal relation between the Stokes velocity and the flocculant concentration: $v_{St} = v_{St}(c)$. The concentration c^{opt} gives the maximal velocity $v_{St}(c^{\text{opt}}) = v_0$.

where we now treat k as a function of ϕ and w :

$$k(\phi, w) = \begin{cases} \tilde{k}, & \text{if } \phi = 0, \\ w/\phi, & \text{otherwise.} \end{cases}$$

We remark that when $\phi = 0$, the value of \tilde{k} is irrelevant, since $w = 0\tilde{k} = 0$, hence both conserved variables are zero. Physically this means that there is no particle that can carry any information of k .

2.3. Feed properties and flocculation. Our goal is to use the property described by k to mark particles by the state of flocculation encountered when entering the CT, expressed in terms of the modulated hindered settling velocity \bar{v}_{hs} (see (7)). Let c denote the dimensionless flocculent concentration (mass of added flocculant per mass suspension). It is well known that the floc size is a unimodal function of the flocculant concentration due to the re-stabilization of particles by flocculant excess. Therefore, the particle settling velocity (Stokes velocity) v_{St} follows the same rule. A typical example of this behavior is shown in Figure 2. Since the function $v_{St}(c)$ is increasing on $[0, c^{\text{opt}}]$, the dimensionless and normalized function

$$\bar{k}(c) := v_{St}(c)/v_0, \quad 0 \leq c \leq c^{\text{opt}},$$

means a one-to-one increasing relation between the flocculant concentration $c \in [0, c^{\text{opt}}]$ and the property $k = \bar{k}(c) \in [v_{\min}/v_0, 1]$. Note that it is sufficient and desired to consider only this increasing relation, since the decreasing part would mean an unnecessary waste of flocculant.

During CT operation, let $\dot{m}_f(t)$ denote the mass of added flocculant per unit time just before the feed inlet to the CT. Then the dimensionless flocculant concentration varies with time according to

$$c(t) = \frac{\dot{m}_f(t)}{\rho_s \phi_f(t) Q_f(t)}, \quad (14)$$

and we define the feed function of the property k as

$$k_f(t) := \bar{k}(c(t)). \quad (15)$$

This function fits exactly in the framework of Section 2.2 and allows us to model the behavior of the CT due to changes in flocculant addition.

3. THICKENING OPERATION AND CONTROL

3.1. Steady-state solutions and operating charts. For the operation of a CT, it is important to establish the dependence of the steady-state solutions on the possible control variables Q_f , Q_u and k_f . Assume that all functions and variables of Equations (8) and (9) are independent of time t . There are steady-state solutions $\phi = \phi(z)$ with solids in the clarification zone, and then the effluent concentration ϕ_e may be positive or zero. If $\phi_e = 0$, then the sediment level, i.e., the position of the interface z_c such that $\phi(z_c) = \phi_c$, is located in the clarification zone. This mode of operation is sometimes called *high-capacity mode* (Bürger and Narváez, 2007). However, here we only consider the most desirable steady-state solutions for which the concentration in the clarification zone is zero (hence $\phi_e = 0$), and for which the sediment level is located in the thickening zone. This means that the feed flux (per area unit) $Q_f\phi_f/A$ equals the flux in the thickening zone. Then Equations (8) and (9) reduce to the following four equalities for the unknowns $\phi(z)$, $k(z)$, ϕ_u , k_u :

$$\frac{Q_f\phi_f}{A} = F(\phi, k) - k \frac{dD(\phi)}{dz} = \frac{Q_u\phi_u}{A}, \quad (16)$$

$$\frac{Q_f k_f \phi_f}{A} = k F(\phi, k) - k^2 \frac{dD(\phi)}{dz} = \frac{Q_u k_u \phi_u}{A}. \quad (17)$$

Assume that $Q_f\phi_f > 0$. Multiplying Equation (16) by k and subtracting Equation (17), we get

$$k(z) - k_f = 0 = k(z) - k_u,$$

which implies that

$$k_f = k = k_u = \text{constant}.$$

Then the left equality of (16) is an equation for the unknown $\phi(z)$; see Bürger and Narváez (2007). It is known that $\phi(z)$ is a non-decreasing function for $0 < z < B$, which may have at most one discontinuity (for physically relevant v_{hs} ; e.g., a sufficient condition is that v_{hs} is decreasing). We are interested in the case when $\phi(B^-) > \phi_c$. This implies that (16) is an ordinary differential equation as long as $\phi > \phi_c$, namely

$$\frac{d\phi}{dz} = \frac{1}{k d(\phi)} \left(F(\phi, k) - \frac{Q_f\phi_f}{A} \right). \quad (18)$$

This equation is easiest integrated from the bottom, with the initial value

$$\phi(B^-) = \phi_u = \frac{Q_f\phi_f}{Q_u}, \quad (19)$$

and upwards to the unique coordinate z_c where the volume fraction has reached the critical concentration, i.e. $\phi(z_c) = \phi_c$. At $z = z_c$, there is a discontinuity above which the solution is constant and equal to ϕ_1 , also called conjugate concentration, which satisfies

$$F(\phi_1, k) = \frac{Q_f \phi_f}{A}.$$

One should bear in mind that, for a given k , there exists a (possibly) small interval of values of the underflow concentration ϕ_u that yield a discontinuity within the thickening zone, i.e. $z_c \in (0, B)$. Furthermore, for a given value of ϕ_u , the location of the discontinuity is influenced by the property k . This relation is well known in dewatering plants and many control systems use this feature to hold the sediment level modifying the flocculant dosage (see, for instance, Furness et al., 1980).

Since at steady state the value of k remains constant, the procedure detailed by Bürger and Narváez (2007) is sufficient to construct a chart of feasible steady states. However, there is no rule that permits us to know *a priori* whether the tuple $(\phi_f, k, \phi_u, \phi_e, Q_f)$ yields an attainable steady state. Usually numerical integration must be used to determine whether a given tuple $(\phi_f, k, \phi_u, \phi_e, Q_f)$ produces a real steady state.

To illustrate the connection between k , ϕ_u and z_c , we consider a CT of 60 m in diameter with $H = 0.8$ m and $B = 3.2$ m. We choose the following constitutive relations, which have been experimentally measured for copper ore tailings by Becker (1982).

$$v_{hs}(\phi) = \begin{cases} 6.05 \cdot 10^{-4} (1 - \phi)^{12.59} \text{ ms}^{-1} & \text{for } 0 \leq \phi \leq 1, \\ 0 & \text{otherwise,} \end{cases}$$

$$\sigma_e(\phi) = \begin{cases} 0 & \text{for } \phi \leq 0.23, \\ 5.35 \exp(17.9\phi) \text{ Pa} & \text{for } \phi > 0.23. \end{cases}$$

The solids have the density $\rho_s = 2650 \text{ kg m}^{-3}$ and the liquid considered here is water ($\rho_f = 1000 \text{ kg m}^{-3}$). For simulations, it will be assumed that the value of v_{St} determined by Becker (1982) corresponds to the maximal value v_0 . We plot contours of $z_c = z_c(k_f, \phi_u)$, with values $Q_f \phi_f = 30, 60$ and $90 \text{ m}^3 \text{ h}^{-1}$. The results are shown in Figure 3.

It can be observed that only a subset of the rectangle $[\phi_c, 1] \times (0, 1]$ yields $z_c \in (0, B)$. This subset represents all possible values for controlling the CT unit under the restriction of no solids in the clarification zone and the sediment level in the thickening zone.

3.2. Thickener Control. In the design of thickener controllers there are two independent variables, flocculant rate and underflow rate. The dependent variables include rake torque, underflow concentration, overflow concentration, sediment level, solids inventory, solids settling rate and underflow viscosity (Schoenbrunn and Toronto, 1999). In the case studied here, we propose to use the underflow rate to control the underflow concentration and the property k_f to control the sediment level. Recalling that $Q_f \phi_f$ in (19) is a given quantity, Q_u can be used as a control variable to obtain a desired ϕ_u (see Diehl, 2008 and Betancourt et al., 2013). For controlling the sediment level, let us suppose that it is possible to manipulate the value of k_f , for instance by modifying the flocculant concentration c . Suppose that $Q_f(t), \phi_f(t)$ are perturbations that cannot be modified. For desired set point values ϕ_u^{SP} and z_c^{SP} , Figure 3 indicates that there exists at most one value of k_f (that we call

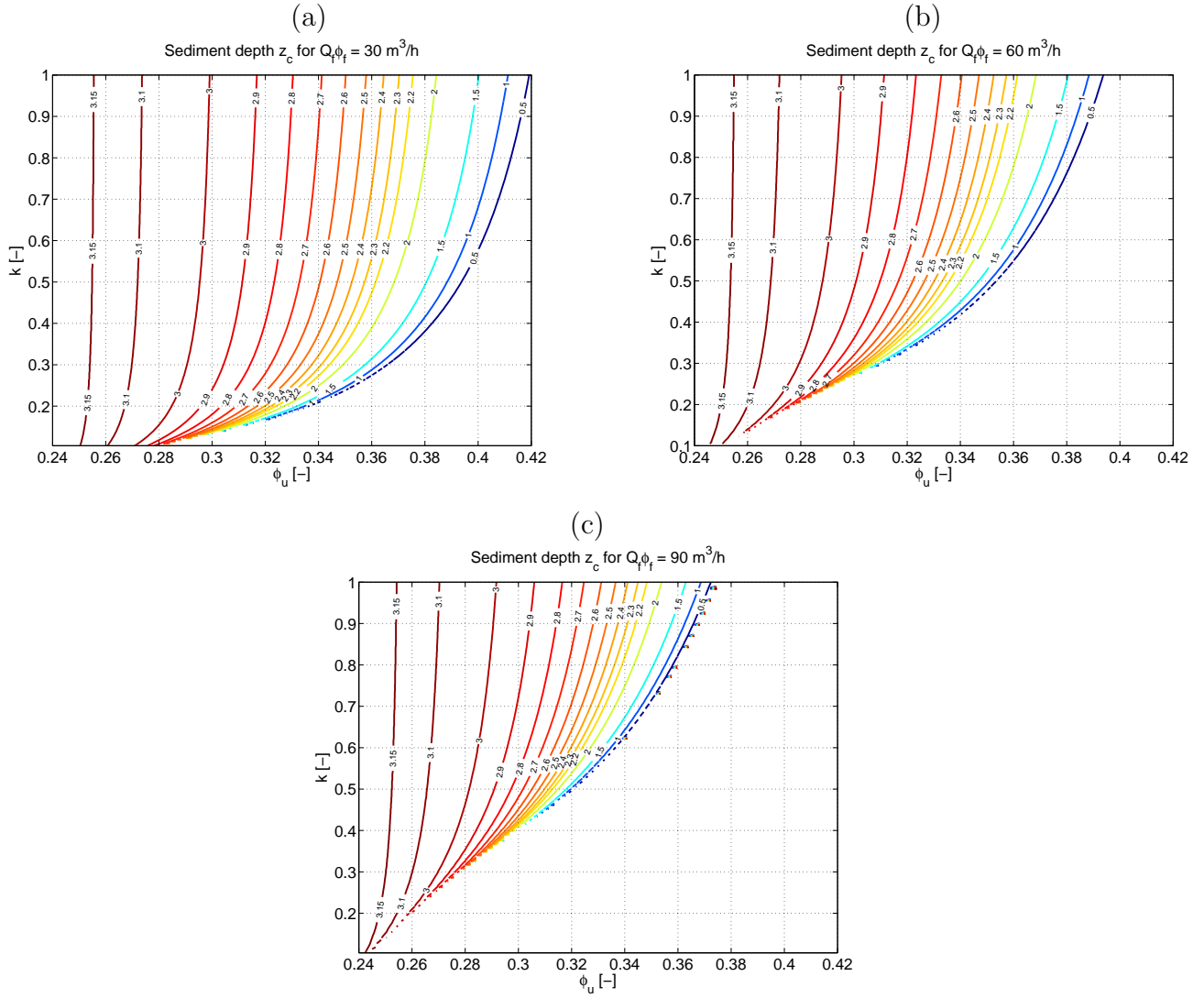


FIGURE 3. Contour plots of the sediment level z_c [m] for $Q_f \phi_f = 30, 60$ and $90 \text{ m}^3/\text{h}$, respectively, which can be used as operating charts for control. Given a desired z_c in steady-state operation, the corresponding curve in a chart gives the possible values of ϕ_u and k in the steady-state solution of the model. When ϕ_u is also chosen, k is given uniquely. Then the control variables are determined by $Q_u = Q_f \phi_f / \phi_u$ and $k_f = k$.

k_f^{SP}) such that the steady-state determined by $(Q_f(t), \phi_f(t), \phi_e = 0, \phi_u^{\text{SP}}, z_c^{\text{SP}})$ is reachable, i.e., $k_f^{\text{SP}} = k_f^{\text{SP}}(Q_f(t), \phi_f(t), \phi_e = 0, \phi_u^{\text{SP}}, z_c^{\text{SP}})$. Consider the following simple proportional

regulator:

$$\begin{aligned} Q_u(t) &= \frac{Q_f(t)\phi_f(t)}{\phi_u^{\text{SP}}} + K_{P1}\overline{\phi_u}(t), \\ k_f(t) &= k_f^{\text{SP}}(\phi_u^{\text{SP}}, z_c^{\text{SP}}) + K_{P2}\overline{z_c}(t), \end{aligned} \tag{20}$$

where we define the deviation variables

$$\begin{aligned} \overline{\phi_u}(t) &:= \phi_u(t) - \phi_u^{\text{SP}}, \\ \overline{z_c} &:= z_c^{\text{SP}} - z_c(t), \end{aligned}$$

and the positive (constant) gains K_{P1} and K_{P2} . The first terms on the right-hand side of (20) contain the steady-state values according to operating charts as in Figure 3. If a deviation is nonzero, the regulator automatically adjusts the control variable in a way that speeds up the transient behaviour of the system towards the given set point values ϕ_u^{SP} and z_c^{SP} . In Section 4, a numerical example showing the improvement in the CT behavior due to the introduction of regulator (20) is presented.

Finally, an operator would like to know the time-variation $c(t)$ (or $\dot{m}_f(t)$) instead of $k_f(t)$, and we have in Section 2.3 described how this can be achieved uniquely.

4. SIMULATIONS

We illustrate the behaviour of the model (8)–(9) (or (12)–(13)) and the possibilities for control of steady states of the CT by two numerical examples. All simulations are performed by the numerical scheme outlined in the Appendix with a cell depth of $\Delta z = 0.003$ m and the tank dimensions and parameter values given in Section 3.1.

4.1. Example 1. We perform three simulations. In all three, we start at steady state with $k_f = 0.5078$, $\phi_f = 0.1500$, $Q_f = 400 \text{ m}^3 \text{ h}^{-1}$ and

$$Q_u = \frac{60}{0.32} \text{ m}^3 \text{ h}^{-1} = 187.5 \text{ m}^3 \text{ h}^{-1},$$

which means that $Q_f\phi_f = 60 \text{ m}^3 \text{ h}^{-1}$ and $\phi_u = 0.32$. As a reference back to the operating charts of Section 3.1, we are positioned on the contour $z_c = 2.65$ m in Figure 3 (b). A step change of the feed flux from $Q_f\phi_f = 60 \text{ m}^3 \text{ h}^{-1}$ to $Q_f\phi_f = 90 \text{ m}^3 \text{ h}^{-1}$ is imposed at time $t = 20$ h by increasing the feed concentration ϕ_f but keeping the volumetric feed flow rate Q_f constant. We thus have to consult Figure 3 (c) to consider the new steady state of the system.

Figure 4 (a) shows the dynamics of the volume fraction ϕ in Simulation 1, during which k_f and Q_u are kept constant. (Since k_f is constant and we start at steady state, $k(z, t) \equiv k_f$ in the thickening zone, we do not show any 3D graph of k .) Clearly the sediment level rises from the thickening zone, through the clarification zone and we end up with a steady-state overflow.

In Simulation 2 (Figure 4 (b)), the previous overflow situation caused by the step increase in the feed flux at $t = 20$ h is prevented by immediately increasing Q_u to $(90/0.32) \text{ m}^3 \text{ h}^{-1}$. This means that we move horizontally to the left in Figure 3 (c) until we meet the underflow volume fraction $\phi_u = 0.32$ keeping $k_f = 0.5078$. The corresponding new contour is $z_c =$

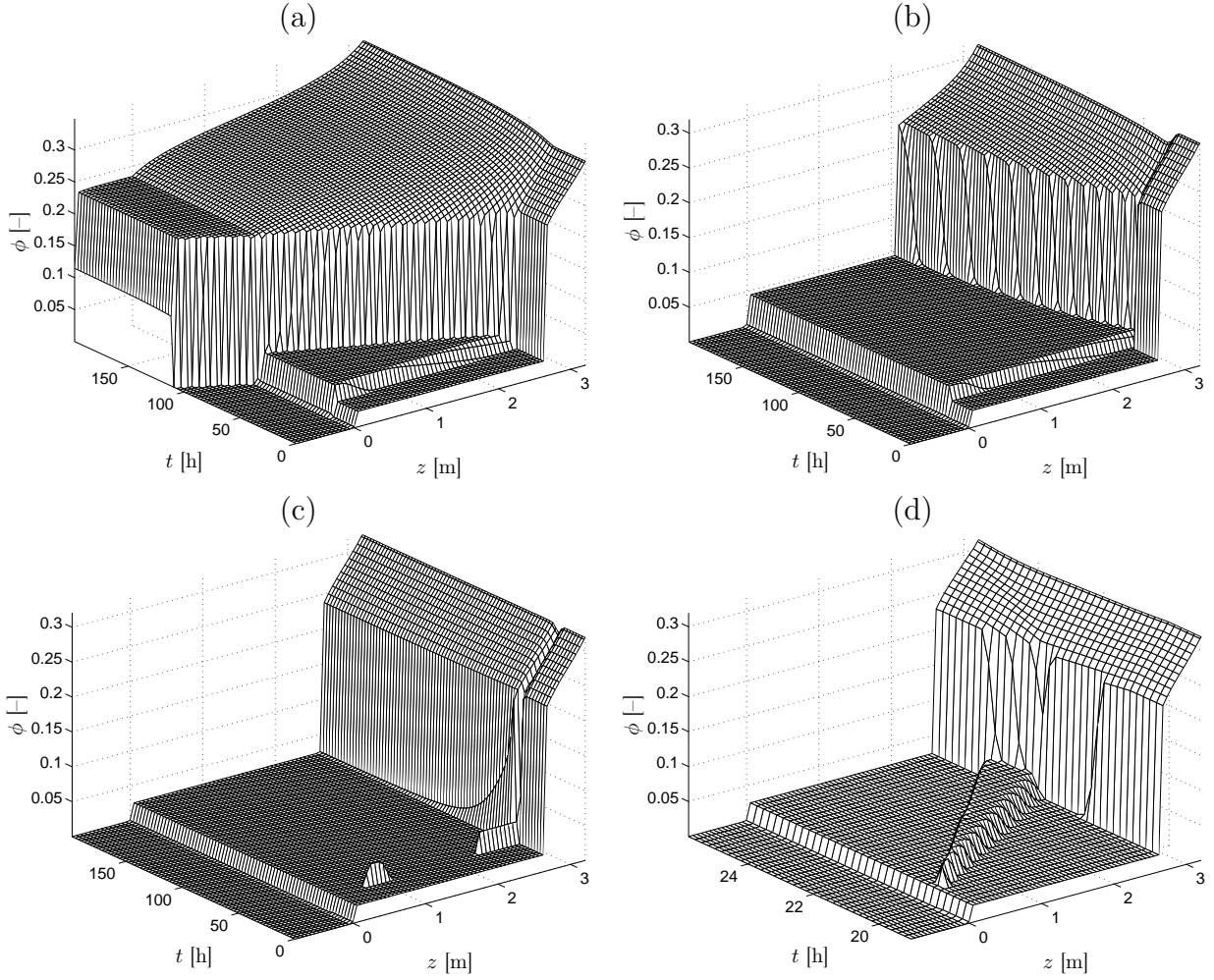


FIGURE 4. (a) Simulation 1: A step increase of the feed flux is imposed at time $t = 50$ h, but no control action is performed. (b) Simulation 2: A step increase of the feed flux is imposed at time $t = 50$ h, k_f is kept constant but Q_u is changed to keep the initial sediment level. (c) Simulation 3: A step increase of the feed flux is imposed at time $t = 50$ h, k_f and Q_u are changed to keep the initial sediment level and underflow volume fraction constant. (d) Zoom of profile in Simulation 3.

1.2441 m. As can be seen in Figure 4 (b), the sediment level rises slowly and it takes a long time to reach this new sediment level.

To keep both z_c and ϕ_u at the same levels as before the disturbance in the feed occurs, it is necessary to change both Q_u and k_f to new values. In Simulation 3, which is shown in Figure 4 (c), this is done by increasing Q_u to $(90/0.32) \text{ m}^3 \text{ h}^{-1}$ and k_f to 0.7615. In Figure 4 (d) a zoom of Figure 4 (c) for $t \in [19, 25]$ is presented. We observe the appearance of a

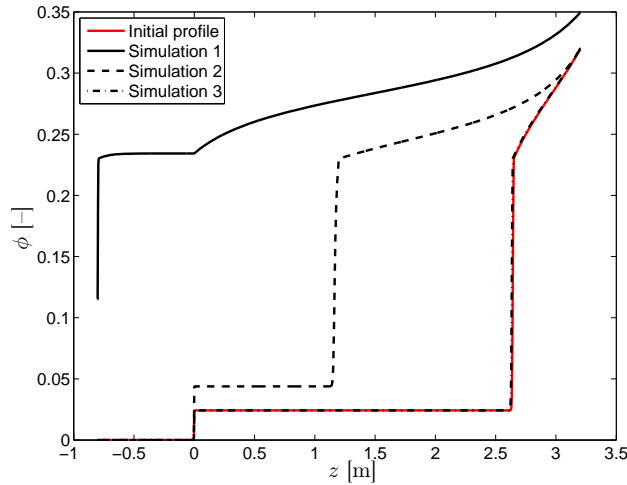


FIGURE 5. The steady state profiles for ϕ ($t = 8000$ h).

wave in the profile due to the collision of incoming particles with greater velocity (i.e. with greater value of k_f) with the slower particles.

It must be noted that the process has not reached steady state in the simulations shown in Figure 4 (a)–(d). The steady-state volume fraction profiles (simulated profiles at time $t = 8000$ h) of all three simulations are shown together with the initial profile in Figure 5.

4.2. Example 2. In Simulation 3 of Example 1, it was shown that a manual control action by immediate changes of Q_u and k_f is sufficient to meet disturbances in the feed stream. Suppose now we wish to introduce a step change in the set point value of z_c . Unfortunately, simulations have shown that this type of manual action gives a very slow convergence to the new reference value (see Figure 6 (a)). In order to improve the performance, the regulator proposed in (20) is connected to the system. This is now demonstrated by two simulations.

In Simulations 4 and 5, we start at a steady state with $k_f = 0.4949$, $\phi_f = 0.15$, $Q_f = 400 \text{ m}^3 \text{ h}^{-1}$ and

$$Q_u = \frac{60}{0.35} \text{ m}^3 \text{ h}^{-1} \approx 171.43 \text{ m}^3 \text{ h}^{-1}.$$

We thus have $Q_f \phi_f = 60 \text{ m}^3 \text{ h}^{-1}$, $\phi_u = 0.35$ and $z_c = 1.0 \text{ m}$. During the first 20 hours, the setpoint values of ϕ_u , z_c and k_f are kept constant equal to the initial values i.e. $\phi_u^{\text{SP}} = 0.35$, $z_c^{\text{SP}} = 1.0 \text{ m}$ and $k_f^{\text{SP}} = 0.4949$. At time $t = 20 \text{ h}$ a step increase in z_c^{SP} to the new value $z_c^{\text{SP}} = 1.5 \text{ m}$ is imposed, which means that we also have to change k_f^{SP} to $k_f^{\text{SP}} = 0.5281$. In Simulation 4, shown in Figures 6 (a) and 7 (a), no controller is connected while in Simulation 5, shown in Figures 6 (b)–(c) and 7 (b), the controller (20) with $K_{P1} = 800 \text{ m}^3 \text{ h}^{-1}$ and $K_{P2} = 0.8$ is used. These gain parameter values have been determined by ad-hoc numerical experiments. The improvement in the response with the controller connected is well visible. On the other hand, the introduction of the controller produces an overshoot in the values of k_f and Q_u (see Figure 6 (c)). This behavior can be attenuated through the incorporation of an integral term in controller (20); however, it would also

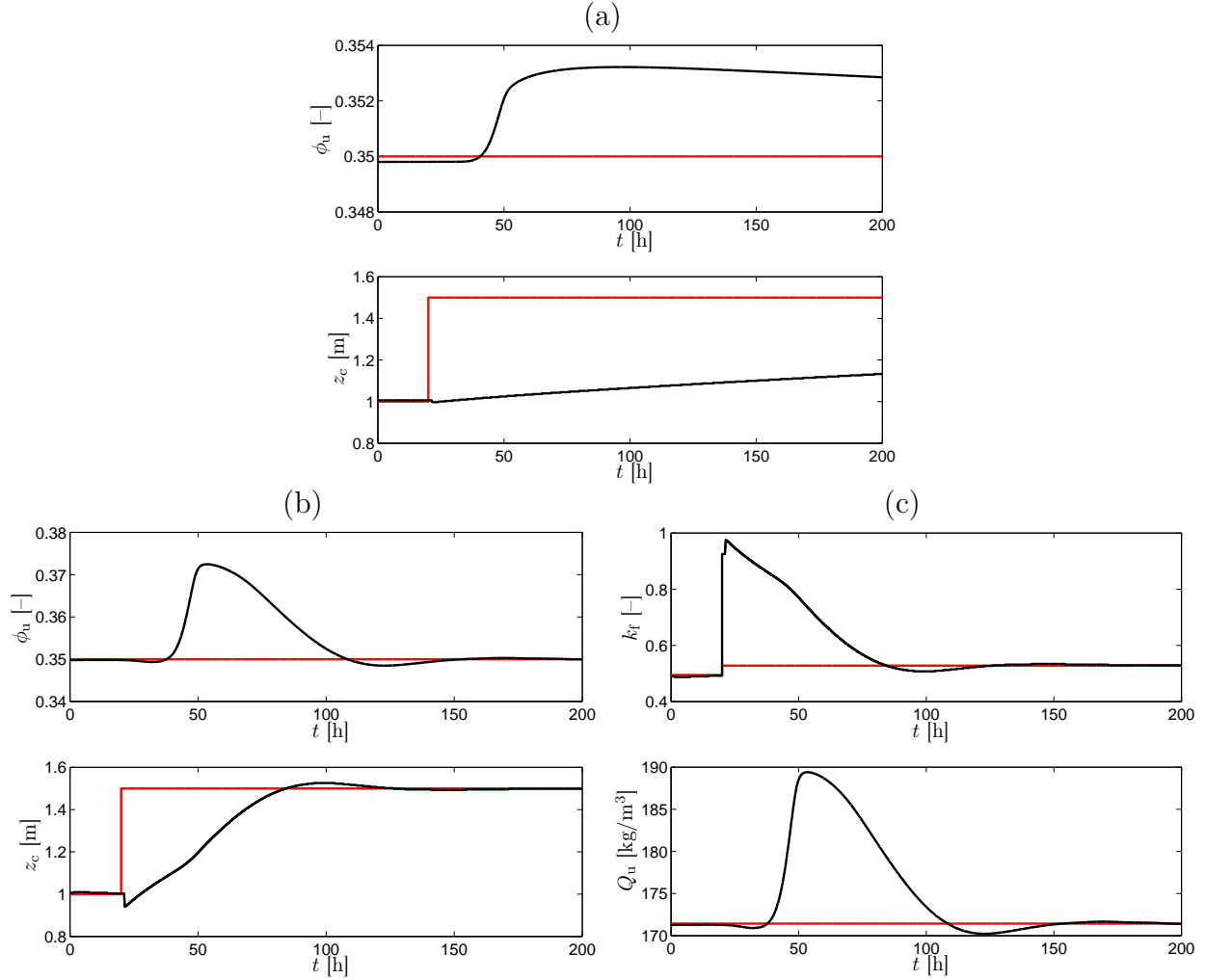


FIGURE 6. Dynamics of different variables (black) and set point values (red). (a) Simulation 4: manual control action of only k_f^{SP} . (b)–(c) Simulation 5: the regulator (20) is used.

incorporate oscillations. The stability properties of this controller is an open question because of the lack of a well-posedness theory for (12)–(13), nevertheless the numerical results show desirable results. The convergence for similar controllers for the model with non-varying feed properties (Subsection 2.1) have been studied by Diehl (2008) and Betancourt et al. (2013).

5. CONCLUSIONS

An extension of an accepted model of a CT is presented together with a simple regulator and a numerical scheme. The model predicts the behavior of a CT under time-varying settling velocity of the solid particles that are fed to the CT. The sediment level appears to be a very sensitive variable with respect to changes in the particle settling velocity. This is in agreement with knowledge from real operation and applied control strategies.

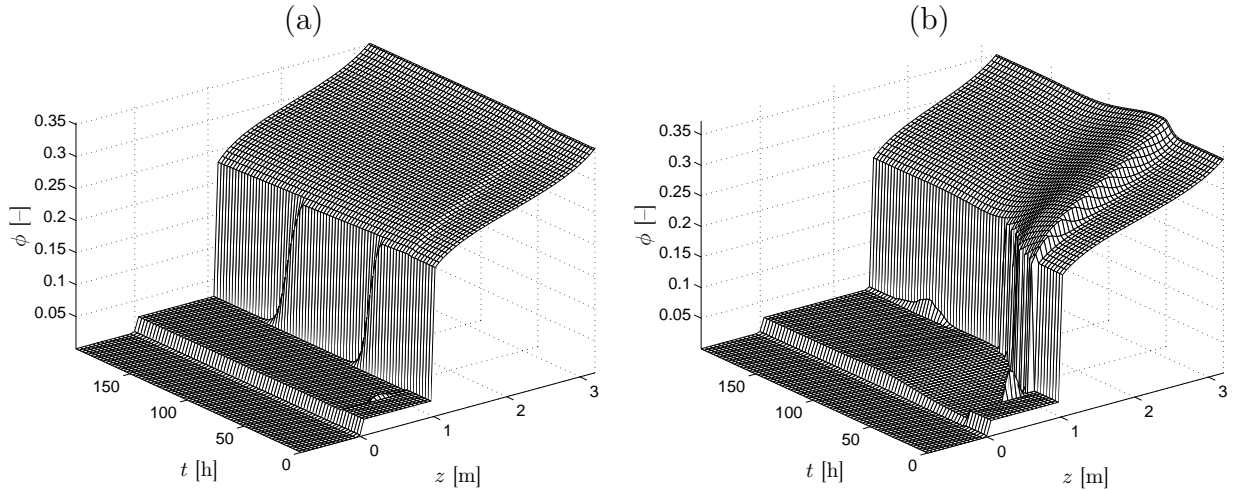


FIGURE 7. Concentration profile of a CT under a change in the set point of sediment level (a) modifying just k_f^{SP} (Simulation 4), (b) connecting the regulator (20) (Simulation 5).

We have shown how manual control of steady states can be made by changing the two control variables Q_u and $k_f(t)$, where the latter in turn can be controlled via addition of a flocculant in the feed stream. The actual values of the control variables are determined by operating charts, which are produced by numerical computations of an ordinary differential equations. This framework facilitates the possibilities of developing more sophisticated controllers for the unit, and already a simple proportional controller improves the transient behaviour substantially.

The well-posedness of the governing equations (12), (13) is a major task, as with any system of conservation laws, and it is out of the scope of the paper. However the numerical results are reasonable with the physics of the problem.

The proposed model is built on the assumption that the suspension is completely flocculated before entering the CT and the model does not consider particle interaction during sedimentation. A more complete model should also include orthokinetic flocculation inside the CT. This effect has been considered, under different assumptions, in wastewater treatment by Lyn et al. (1992).

ACKNOWLEDGEMENTS

FB acknowledges support by Conicyt Programm “Inserción de Capital Humano Avanzado en la Academia” 791100041. RB is supported by Fondecyt project 1130154; BASAL project CMM, Universidad de Chile and Centro de Investigación en Ingeniería Matemática (CI²MA), Universidad de Concepción; Conicyt project Anillo ACT1118 (ANANUM); and Red Doctoral REDOC.CTA, MINEDUC project UCO1202 at Universidad de Concepción. SF gratefully acknowledges the Crafoord foundation, Sweden (grant 20110535).

APPENDIX

We divide the spatial axis in cells of depth $\Delta z > 0$ and define the grid points $z_j := j\Delta z$ and the staggered grid points $z_{j+1/2} := (j + 1/2)\Delta z$ for $j = 0, \pm 1, \dots$. Similarly, the time axis is discretized at the points $t^n := n\Delta t$ for $n = 0, 1, \dots$ with the time step length $\Delta t > 0$. We consider the cell averages of the conserved properties ϕ and w on each cell $[z_{j-1/2}, z_{j+1/2}]$:

$$\phi_j^n := \frac{1}{\Delta z} \int_{z_{j-1/2}}^{z_{j+1/2}} \phi(z, t^n) dz \quad \text{and} \quad w_j^n := \frac{1}{\Delta z} \int_{z_{j-1/2}}^{z_{j+1/2}} w(z, t^n) dz,$$

while q and γ are considered on the staggered grid:

$$q_{j+1/2}^n := \frac{1}{\Delta z} \int_{z_j}^{z_{j+1}} q(z, t^n) dz = q(z_{j+1/2}, t^n) \quad \text{and} \quad \gamma_{j+1/2}^n := \frac{1}{\Delta z} \int_{z_j}^{z_{j+1}} \gamma(z) dz.$$

The numerical scheme consists of two steps via an operator splitting, where the linear and nonlinear contributions to the fluxes are considered separately. With the notation $\mathbf{u}_j^n := (\phi_j^n, w_j^n)$, $\mathbf{u}_f^n := (\phi_f^n, w_f^n)$ and $\lambda := \Delta t / \Delta z$, the first step of the scheme reads

$$\mathbf{u}_j^{n+1/2} = \mathbf{u}_j^n - \lambda \left(q_{j+1/2}^{n,-} (\mathbf{u}_{j+1}^n - \mathbf{u}_f^n) + (q_{j+1/2}^{n,+} - q_{j-1/2}^{n,-}) (\mathbf{u}_j^n - \mathbf{u}_f^n) - q_{j-1/2}^{n,+} (\mathbf{u}_{j-1}^n - \mathbf{u}_f^n) \right),$$

where $q_{j+1/2}^{n,+} := \max(q_{j+1/2}^n, 0)$ and $q_{j+1/2}^{n,-} := \min(q_{j+1/2}^n, 0)$. This update from the linear bulk fluxes is then used to approximate the nonlinear fluxes by first computing

$$k_j^{n+1/2} := \begin{cases} \tilde{k} & \text{if } \phi_j^{n+1/2} = 0, \\ w_j^{n+1/2} / \phi_j^{n+1/2} & \text{otherwise,} \end{cases}$$

and

$$\mathcal{V}_{j+1/2}^{n+1/2} := \gamma_{j+1/2} k_{j+1}^{n+1/2} v_{\text{hs}}(\phi_{j+1}^{n+1/2}).$$

The second step of the scheme is

$$\begin{aligned} \phi_j^{n+1} &= \phi_j^{n+1/2} - \lambda (\mathcal{V}_{j+1/2}^{n+1/2} \phi_j^{n+1/2} - \mathcal{V}_{j-1/2}^{n+1/2} \phi_{j-1}^{n+1/2}) \\ &\quad + \mu \left(\gamma_{j+1/2} w_{j+1/2}^{n+1/2} [D_1(\phi_{j+1}^{n+1/2}) - D_1(\phi_j^{n+1/2})] \right. \\ &\quad \left. - \gamma_{j-1/2} w_{j-1/2}^{n+1/2} [D_1(\phi_j^{n+1/2}) - D_1(\phi_{j-1}^{n+1/2})] \right), \\ w_j^{n+1} &= w_j^{n+1/2} - \lambda (\mathcal{V}_{j+1/2}^{n+1/2} w_j^{n+1/2} - \mathcal{V}_{j-1/2}^{n+1/2} w_{j-1}^{n+1/2}) \\ &\quad + \mu \left(\gamma_{j+1/2} (w_{j+1/2}^{n+1/2})^2 [D_2(\phi_{j+1}^{n+1/2}) - D_2(\phi_j^{n+1/2})] \right. \\ &\quad \left. - \gamma_{j-1/2} (w_{j-1/2}^{n+1/2})^2 [D_2(\phi_j^{n+1/2}) - D_2(\phi_{j-1}^{n+1/2})] \right), \end{aligned}$$

where $\mu := \lambda / \Delta z$ and

$$w_{j+1/2}^{n+1/2} := \begin{cases} \min\{w_j^{n+1/2}, \phi_{j+1}^{n+1/2}\} & \text{if } \phi_{j+1}^{n+1/2} \leq \phi_j^{n+1/2}, \\ \min\{w_{j+1}^{n+1/2}, \phi_j^{n+1/2}\} & \text{otherwise.} \end{cases} \quad (\text{A.1})$$

The following CFL condition has been used:

$$\max\{C_1, C_2, C_3\} \leq 1,$$

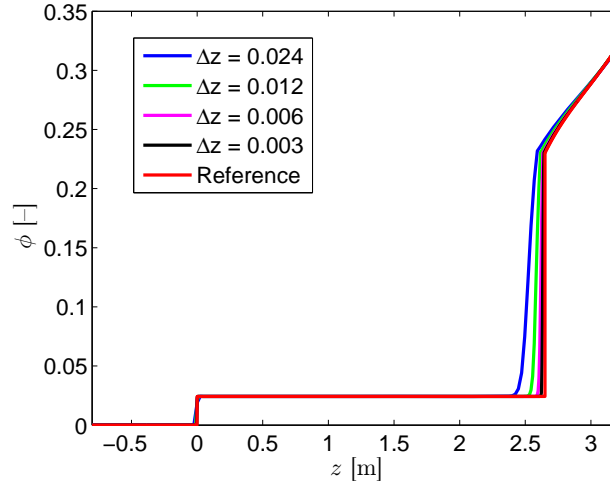


FIGURE 8. Convergence test of the numerical scheme.

where

$$C_1 = \lambda \max_{0 \leq t \leq T} \frac{Q_e(t) + Q_u(t)}{A},$$

$$C_2 = \lambda \max_{0 \leq \phi \leq 1} (v_{\text{hs}}(\phi) - \phi v'_{\text{hs}}(\phi)) + 2\mu \max_{0 < \phi \leq 1} \frac{d(\phi)}{\phi},$$

$$C_3 = \lambda \max_{0 \leq \phi \leq 1} v_{\text{hs}}(\phi) + 4\mu \max_{0 < \phi \leq 1} \frac{d(\phi)}{\phi^2},$$

and T is the total simulation time. The convergence of the scheme as $\Delta z \rightarrow 0$ is tested numerically by running Simulation 3 with different values of Δz ; see Figure 8.

REFERENCES

- Aziz, A.A.A., de Kretser, R.G., Dixon, D.R. and Scales, P.J., 2000. The characterisation of slurry dewatering. *Water Science and Technology* 41(8), 9–16.
- Barton, N.G., Li, C.-H. and Spencer, J., 1992. Control of a Surface of Discontinuity in Continuous Thickeners. *Journal of Australian Mathematical Society Series B*, 33, 269–289.
- Balastre, M., Argillier, J.F., Allain, C. and Foissy, A., 2002. Role of polyelectrolyte dispersant in the settling behavior of a barium sulphate suspension. *Colloids and Surfaces A: Physicochemical and Engineering Aspects* 211, 145–156.
- Becker, R., 1982. *Espesamiento Continuo, Diseño y Simulación de Espesadores*. Habilitación Profesional, Universidad de Concepción, Chile.
- Besra, L., Singh, B.P., Reddy, P.S.R., Sengupta, D.K., and Bhoumik, S.K., 1996. Effect of flocculant on settling and filtration of iron-ore sludge. *Minerals and Metallurgical Processing* 13, 170–173.

- Betancourt, F., Concha, F. and Sbárbaro, D., 2013. Simple mass balance controllers for continuous sedimentation. *Computers & Chemical Engineering* 54, 34–43.
- Bürger, R., Diehl, S., Farås, S. and Nopens, I., 2012. On reliable and unreliable numerical methods for the simulation of secondary settling tanks in wastewater treatment. *Computers & Chemical Engineering* 41, 93–105.
- Bürger, R., Diehl, S., Farås, S., Nopens, I. and Torfs, E., 2013. A consistent modelling methodology for secondary settling tanks: a reliable numerical method. *Water Science and Technology* 68, 192–208.
- Bürger, R., Diehl, S. and Nopens, I., 2011. A consistent modelling methodology for secondary settling tanks in wastewater treatment. *Water Research* 45, 2247–2260.
- Bürger, R., Karlsen, K.H. and Towers, J.D., 2005. A model of continuous sedimentation of flocculated suspensions in clarifier-thickener units. *SIAM Journal on Applied Mathematics* 65, 882–940.
- Bürger, R. and Narváez, A., 2007. Steady-state, control, and capacity calculations for flocculated suspensions in clarifier-thickeners. *International Journal of Mineral Processing* 84, 274–298.
- Bustos, M.C., Concha, F. and Wendland, W.L., 1990a. Global weak solutions to the problem of continuous sedimentation of an ideal suspension. *Mathematical Methods in the Applied Sciences* 13, 1–22.
- Bustos, M.C., Paiva, F. and Wendland, W.L., 1990b. Control of continuous sedimentation of ideal suspensions as an initial and boundary value problem. *Mathematical Methods in the Applied Sciences* 12, 533–548.
- Bustos, M.C., Concha, F., Bürger, R. and Tory, E.M., 1999. *Sedimentation and Thickening*. Kluwer Academic Publishers, Dordrecht, The Netherlands.
- Chakrabarti, S., Banerjee, S., Chaudhuri, B., Bhattacharjee, S. and Dutta, B.K., 2008. Application of biodegradable natural polymers for flocculated sedimentation of clay slurry. *Bioresource Technology* 99, 3313–3317.
- Chancelier, J.-Ph., Cohen de Lara, M. and Pacard, F., 1994. Analysis of a Conservation PDE with Discontinuous Flux: A Model of Settler. *SIAM Journal of Applied Mathematics*, 54(4), 954–995.
- Chen, Y., Liu, S. and Wang, G., 2007. A kinetic investigation of cationic starch adsorption and flocculation in kaolin suspension. *Chemical Engineering Journal* 133, 325–333.
- Concha, F. and Barrientos, A., 1993. A critical review of thickener design methods. *KONA Powder and Particle* 11, 79–104.
- Concha, F. and Bürger, R., 2002. A century of research in sedimentation and thickening. *KONA Powder and Particle* 20, 38–70.
- Concha, F. and Bürger, R., 2003. Thickening in the 20th century: a historical perspective. *Minerals and Metallurgical Processing* 20, 57–67.
- Concha, F., and Bustos, M. C., 1992. Settling velocities of particulate systems, 7. Kynch sedimentation processes: continuous thickening. *International journal of mineral processing* 34, 33–51.
- Diehl, S., 2006. Operating charts for continuous sedimentation III: Control of step inputs. *Journal of Engineering Mathematics*, 54, 225–259.

- Diehl, S., 2008. A regulator for continuous sedimentation in ideal clarifier-thickener units. *Journal of Engineering Mathematics* 60, 265–291.
- Diehl, S., 2012. Shock-wave behaviour of sedimentation in wastewater treatment: a rich problem. In Åström, K.m Persson, L.-E. and Silvestrov, S.D. (Eds.), *Analysis for Science, Engineering and Beyond*. Springer Proceedings in Mathematics vol. 6, Springer, Berlin, 175–214.
- Diehl, S. and Farås, S., 2013. Control of an ideal activated sludge process in wastewater treatment via an ODE-PDE model. *Journal of Process Control*, 23, 359–381.
- Eswaraiah, C., Biswal, S.K. and Mishra, B.K., 2012. Settling characteristics of ultrafine ore slimes. *International Journal of Minerals, Metallurgy and Materials* 19, 95–99.
- Fitch, E.B., 1993. Gravity Separation Operations. In McKetta, J.J. (Ed.), *Unit Operations Handbook* vol. 2, Marcel Dekker Inc., New York, 51–127.
- Furness, K.M., Quiñonez, M. and Low, S.T., 1980. Thickener control system. US Patent 4226714, October 7, 1980.
- Garrido, P., Bürger, R. and Concha, F., 2000. Settling velocities of particulate systems: 11. Comparison of the phenomenological sedimentation-consolidation model with published experimental results. *International Journal of Mineral Processing* 60, 213–227.
- Glover, S.M., Yan, Y., Jameson, G.J. and Biggs, S., 2000. Bridging flocculation studied by light scattering and settling. *Chemical Engineering Journal* 80, 3–12.
- Glover, S.M., Yan, Y., Jameson, G.J. and Biggs, S., 2004. Dewatering properties of dual-polymer-flocculated systems. *International Journal of Mineral Processing* 73, 145–160.
- Gregory, J., 2005. *Particles in Water: Properties and Processes*. CRC Press, Boca Raton, FL, USA.
- Hogg, R., 2000. Flocculation and dewatering. *International Journal of Mineral Processing* 58, 223–236.
- Hogg, R., 2013. Bridging flocculation by polymers. *KONA Powder and Particle* 30, 3–14.
- Jin, B., Wilén, B.-M. and Lant, P., 2003. A comprehensive insight into floc characteristics and their impact on compressibility and settle ability of activated sludge. *Chemical Engineering Science* 95, 221–234.
- Kourki, H. and Famili, M.H.N., 2012. Particle sedimentation: effect of polymer concentration on particle-particle interaction. *Powder Technology* 221, 137–143.
- Kynch, G.J., 1952. A theory of sedimentation. *Transactions of the Faraday Society* 48, 166–176.
- Lester, D.R., Rudman, M. and Scales, P.J., 2010. Macroscopic dynamics of flocculated colloidal suspensions. *Chemical Engineering Science* 65, 6362–6378.
- Lyn, D., Stamou, A. and Rodi, W., 1992. Density currents and shear-induced flocculation in sedimentation tanks. *Journal of Hydraulic Engineering* 118, 849–867.
- McFarlane, A., Bremmell, K. and Addai-Mensah, J., 2005. Microstructure, rheology and dewatering behaviour of smectite dispersions during orthokinetic flocculation. *Minerals Engineering* 18, 1173–1182.

- McGuire, M.J., Addai-Mensah, J. and Bremmell, K., 2008. Improved dewaterability of iron oxide dispersions: the role of polymeric flocculant type, pH and shear. *Asia-Pacific Journal of Chemical Engineering* 3, 18–23.
- Osborne, D.G., 1981. Gravity thickening. In Svarovsky, L. (Ed.), *Solid-Liquid Separation*, 2nd ed., Butterworths, London, 120–161.
- Perry, R.H., Green, D.W. and Maloney, J.O., 1998. *Perry's Chemical Engineers' Handbook*, Seventh Edition. McGraw-Hill, New York.
- Petty, C.A., 1975. Continuous sedimentation of a suspension with a nonconvex flux law. *Chemical Engineering Science* 30, 1451–1458.
- Richardson, J.F. and Zaki, W.N., 1954. Sedimentation and fluidization: part I. *Transactions of the Institution of Chemical Engineers (London)* 32, 35–53.
- Schoenbrunn, F. and Toronto, T., 1999. Advanced thickener control. In: *Advanced Process Control Applications for Industry Workshop, 1999*. IEEE Industry Applications Society, 83–86.
- Schoenbrunn, F. and Laros, T., 2002. Design features and types of sedimentation equipment. *Mineral Processing Plant Design, Practice, and Control: Proceedings, Vol. 2*, 1331.
- Shannon, P.T. and Tory, E.M., 1966. The analysis of continuous thickening. *SME Transactions* 235, 375–382.
- Wills, B.A. and Napier-Munn, T. (eds.), 2006. *Wills' Mineral Processing Technology*. Seventh Edition. Butterworth-Heinemann/Elsevier, Oxford, UK.
- Ye, X., Tong, P. and Fetteers, L.J., 1998. Colloidal sedimentation in polymer solutions. *Macromolecules* 31, 6534–6540.
- Zhao, Y.Q., 2004. Settling behavior of polymer flocculated water-treatment sludge I: analyses of settling curves. *Separation and Purification Technology* 35, 71–80.

Centro de Investigación en Ingeniería Matemática (CI²MA)

PRE-PUBLICACIONES 2013

- 2013-07 RICARDO OYARZÚA, DOMINIK SCHÖTZAU: *An exactly divergence-free finite element method for a generalized Boussinesq problem*
- 2013-08 HERNÁN MARDONES, CARLOS M. MORA: *Stable numerical methods for two classes of SDEs with multiplicative noise: bilinear and scalar*
- 2013-09 ALFREDO BERMÚDEZ, DOLORES GÓMEZ, RODOLFO RODRÍGUEZ, PABLO VENEGAS: *Mathematical and numerical analysis of a transient non-linear axisymmetric eddy current model*
- 2013-10 ANA ALONSO-RODRIGUEZ, JESSIKA CAMAÑO, RODOLFO RODRÍGUEZ, ALBERTO VALLI: *A posteriori error estimates for the problem of electrostatics with a dipole source*
- 2013-11 ZHIXING FU, LUIS F. GATICA, FRANCISCO J. SAYAS: *Matlab tools for HDG in three dimensions*
- 2013-12 SALIM MEDDAHI, DAVID MORA, RODOLFO RODRÍGUEZ: *A finite element analysis of a pseudostress formulation for the Stokes eigenvalue problem*
- 2013-13 GABRIEL CARCAMO, FABIÁN FLORES-BAZÁN: *A geometric characterization of strong duality in nonconvex quadratic programming with linear and nonconvex quadratic constraints*
- 2013-14 RAIMUND BÜRGER, CHRISTOPHE CHALONS, LUIS M. VILLADA: *Anti-diffusive and random-sampling Lagrangian-remap schemes for the multi-class Lighthill-Whitham-Richards traffic model*
- 2013-15 FERNANDO BETANCOURT, RAIMUND BÜRGER, STEFAN DIEHL, CAMILO MEJÍAS: *Advance methods of flux identification for Clarifier-Thickener simulation models*
- 2013-16 FABIÁN FLORES-BAZÁN: *A Fritz John necessary optimality condition of the alternative-type*
- 2013-17 VERONICA ANAYA, DAVID MORA, RICARDO RUIZ-BAIER: *An augmented mixed finite element method for the vorticity-velocity-pressure formulation of the Stokes equations*
- 2013-18 FERNANDO BETANCOURT, RAIMUND BÜRGER, STEFAN DIEHL, SEBASTIAN FARÁS: *A model of clarifier-thickener control with time-dependent feed properties*

Para obtener copias de las Pre-Publicaciones, escribir o llamar a: DIRECTOR, CENTRO DE INVESTIGACIÓN EN INGENIERÍA MATEMÁTICA, UNIVERSIDAD DE CONCEPCIÓN, CASILLA 160-C, CONCEPCIÓN, CHILE, TEL.: 41-2661324, o bien, visitar la página web del centro: <http://www.ci2ma.udec.cl>



**CENTRO DE INVESTIGACIÓN EN
INGENIERÍA MATEMÁTICA (CI²MA)
Universidad de Concepción**



Casilla 160-C, Concepción, Chile
Tel.: 56-41-2661324/2661554/2661316
<http://www.ci2ma.udec.cl>

